Agriculture, Ecosystems and Environment 249 (2017) 57–69

Contents lists available at ScienceDirect

Agriculture, Ecosystems and Environment

journal homepage: www.elsevier.com/locate/agee

Nitrous oxide emissions from winter oilseed rape cultivation

Reiner Ruser[a,*], Roland Fuß[b], Monique Andres[c], Hannes Hegewald[d], Katharina Kesenheimer[a], Sarah Köbke[e], Thomas Räbiger[f], Teresa Suarez Quinones[g], Jürgen Augustin[c], Olaf Christen[d], Klaus Dittert[e], Henning Kage[f], Iris Lewandowski[h], Annette Prochnow[g,i], Heinz Stichnothe[j], Heinz Flessa[b]

[a] Institute of Crop Science, Department Fertilization and Soil Matter Dynamics, University Hohenheim (340i), Fruwirthstraße 20, D-70599, Stuttgart, Germany
[b] Thünen Institute of Climate-Smart Agriculture, Bundesallee 50, D-38116, Braunschweig, Germany
[c] Institute of Landscape Biogeochemistry, Leibniz Centre for Agricultural Landscape Research (ZALF), Eberswalder Straße 84, D- 15374, Müncheberg, Germany
[d] Institute of Agricultural and Nutritional Sciences, Martin-Luther-University Halle-Wittenberg, Betty-Heimann-Straße 5, D-06120, Halle, Germany
[e] Institute of Applied Plant Nutrition, Georg-August-Universität Göttingen, Carl-Sprengel-Weg 1, D-37075, Göttingen, Germany
[f] Institute of Crop Science and Plant Breeding, Christian-Albrechts-University Kiel, Hermann-Rodewald-Str. 9, D-24118, Kiel, Germany
[g] Leibniz Institute for Agricultural Engineering and Bioeconomy (ATB Bornim), Max-Eyth-Allee 100, D-14469, Potsdam, Germany
[h] Institute of Crop Science, Department Biobased Products and Energy Crops, University Hohenheim (340b), Fruwirthstraße 23, D-70599, Stuttgart, Germany
[i] Faculty of Life Sciences, Humboldt University of Berlin, Hinter der Reinhardtstraße 8-18, D-10115, Berlin, Germany
[j] Thünen Institute of Agricultural Technology, Bundesallee 50, D-38116, Braunschweig, Germany

ABSTRACT

Winter oilseed rape (*Brassica napus* L., WOSR) is the major oil crop cultivated in Europe. Rapeseed oil is predominantly used for production of biodiesel. The framework of the European Renewable Energy Directive requires that use of biofuels achieves GHG savings of at least 50% compared to use of fossil fuel starting in 2018. However, N_2O field emissions are estimated using emission factors that are not specific for the crop and associated with strong uncertainty. N_2O field emissions are controlled by N fertilization and dominate the GHG balance of WOSR cropping due to the high global warming potential of N_2O. Thus, field experiments were conducted to increase the data basis and subsequently derive a new WOSR-specific emission factor.

N_2O emissions and crop yields were monitored for three years over a range of N fertilization intensities at five study sites representative of German WOSR production. N_2O fluxes exhibited the typical high spatial and temporal variability in dependence on soil texture, weather and nitrogen availability. The annual N_2O emissions ranged between 0.24 kg and 5.48 kg N_2O-N ha^{-1} a^{-1}. N fertilization increased N_2O emissions, particularly with the highest N treatment (240 kg N ha^{-1}). Oil yield increased up to a fertilizer amount of 120 kg N ha^{-1}, higher N-doses increased grain yield but decreased oil concentrations in the seeds. Consequently oil yield remained constant at higher N fertilization. Since, yield-related emission also increased exponentially with N surpluses, there is potential for reduction of the N fertilizer rate, which offers perspectives for the mitigation of GHG emissions.

Our measurements double the published data basis of annual N_2O flux measurements in WOSR. Based on this extended dataset we modeled the relationship between N_2O emissions and fertilizer N input using an exponential model. The corresponding new N_2O emission factor was 0.6% of applied fertilizer N for a common N fertilizer amount under best management practice in WOSR production (200 kg N ha^{-1} a^{-1}). This factor is substantially lower than the linear IPCC Tier 1 factor (EF1) of 1.0% and other models that have been proposed.

1. Introduction

In the context of biofuel production especially nitrous oxide (N_2O) contributes to high GHG emissions during the step of biomass production (Dufossé et al., 2013; Hong, 2012). N_2O is a climate relevant trace gas that absorbs light in the IR spectrum and therefore reduces the atmospheric transparency to thermal radiation from the earth's surface (Granli and Bøckman, 1994). The atmospheric N_2O concentration in the last decade increased by 0.73 ppb a^{-1} and with a mean concentration of 328 ppb in 2015 it exceeded the pre-industrial level by about 21%

* Corresponding author.
E-mail address: reiner.ruser@uni-hohenheim.de (R. Ruser).

http://dx.doi.org/10.1016/j.agee.2017.07.039
Received 23 February 2017; Received in revised form 28 July 2017; Accepted 29 July 2017
Available online 24 August 2017

(WMO, 2016). N_2O contributes 7.4% (0.17 W m^{-2}) of the total anthropogenic radiative forcing (IPCC, 2013); it has a high heat adsorption capacity, a long atmospheric lifetime of more than 100 years and has a 296 fold higher global warming potential (IPCC, 2001; RED, 2009) compared to the same mass of carbon dioxide (CO_2). Besides its contribution to the greenhouse effect, N_2O also contributes to stratospheric ozone depletion (Crutzen, 1981; Ravishankara et al., 2009).

Approximately 60% of anthropogenic N_2O emissions are released by agricultural soils (Clais et al., 2013). There is general agreement that nitrification and biological denitrification are the main sources for N_2O production in soils (Bremner, 1997), whereas the contribution of other processes such as nitrifier-denitrification is currently under discussion (Wrage et al., 2001; Shaw et al., 2006; Butterbach-Bahl et al., 2013).

All processes of N_2O production in soils rely on mineral N (i.e. Ruser et al., 2001; Zebarth et al., 2008). Therefore, N_2O emissions from agricultural soils generally increase with increasing N fertilization as it provides the substrates (NO_3^-, NH_4^+) for N_2O production (i.e. Stehfest and Bouwman, 2006). Furthermore, N_2O emission is correlated with N surpluses (N fertilization – N removal) in arable systems (Kaiser and Ruser, 2001; Van Groenigen et al., 2004) as well as in horticultural systems (Pfab et al., 2011).

Oilseed rape (*Brassica napus* L.) is the major oil crop in Europe, accounting for more than 70% of the European oilseed volume in 2012 (Carré and Pouzet, 2014). In 2014, oilseed rape covered 9.1 × 10^6 ha or approximately 8.5% of the total European arable land (FAO, 2016). The corresponding mean grain yield was 3.17 Mg ha^{-1}. In the same year, the mean grain yield in Germany was 4.48 Mg ha^{-1} on 1.4 × 10^6 ha (German Federal Statistical Office, 2017), showing both the high potential for winter oilseed rape (WOSR) cultivation as well as the reason for Germany's leading position (together with France) regarding WOSR production in the EU.

The acreage of WOSR in the European Union more than doubled between 2003 and 2014 (FAO, 2016), which went along with the increase of biodiesel contributing more than 75% of the transport biofuels in Europe (Hamelinck et al., 2013). This increased production is also a result of the Renewable Energy Directive (RED, 2009), in which the European Union mandates a share of 10% from renewables in the transport energy sector by 2020. The RED also defined sustainability criteria for biofuels, which were updated in 2015 (EU, 2015). According to these criteria, biofuels can only be considered and consequently subsidized as such if they contribute to a total reduction of greenhouse gas emissions (GHG) of 35% (current reduction value) and, starting from 2018, of 50% (for production plants that became operational before October 2015) and by 60% (for new production plants) in comparison to the use of fossil fuel.

WOSR is a crop demanding high amounts of N fertilizer to build up efficient photosynthetic leaf tissue (Hegewald et al., 2016). Maximum yields are often achieved with N rates exceeding 200 kg N ha^{-1} whereas N removal with the seeds as well as the N harvest index are low, thereby resulting in high N surpluses of up to 90 kg N ha^{-1} a^{-1} (Henke et al., 2007; Sieling and Kage, 2010). It has also been reported that large amounts of crop residues (petals and leaves), which can be mineralized easily, are returned to the soil after flowering (Sieling and Kage, 2010). Furthermore, N uptake by WOSR plants ends early and increases in N content in seeds during pod filling is more the result of N translocation from vegetative plant parts than from N uptake from soil (Malagoli et al., 2005); both will result in enhanced soil mineral N contents during or shortly after the harvest period. Winter wheat (*Triticum aestivum* L.) is the predominant succeeding crop for WOSR in German crop rotations. The N uptake of winter wheat before winter is approximately 20 kg N ha^{-1} and as such markedly below the N release after WOSR cultivation (Sieling and Kage, 2010). Both, the N surpluses as well as the high soil nitrate contents have the potential of fueling N_2O production in soils.

Due to the high global warming potential of N_2O, the assessment of N_2O emissions with a reliable emission factor is of vital importance for the calculation of GHG balances of biofuels, such as biodiesel produced from WOSR. Results from life cycle analysis (LCA) suggest that direct and indirect N_2O emissions account for between 20 and 40% of the total GHG emission associated with the production and consumption of biodiesel (Hong, 2012; Dufossé et al., 2013). For a bioethanol production system, the choice of different available N_2O emission factors in LCAs might result in completely contrasting results and conclusions, as Smith and Searchinger (2012) remarkably demonstrated. Following IPCC guidance, they set the emission factor to 1.5% (including direct and indirect emissions) and the corresponding emission reached the 35% GHG reduction goal. Using the distinct higher emission factor of 4%, as suggested by Crutzen et al. (2008), based on their so called "top-down" approach, the reduction potential for wheat-based bioethanol was completely eliminated.

In order to assess fertilizer-induced N_2O emissions, different N_2O emission factors have been proposed. The IPCC (2006) guidelines suggest a constant direct N_2O-N loss of 1% of N applied and N in crop residues. This default emission factor was modified from a global data set for wheat and grassland sites originally provided by Bouwman (1996) and, as mentioned by Bouwman, does not consider crop type or site-specific effects. A further drawback of this emission factor is that N_2O emissions do not necessarily correlate linearly with N fertilizer amounts and that N_2O emissions increase over-proportionally when high N fertilizer doses exceed plant demand (McSwiney and Robertson, 2005; Hoben et al., 2011; Kim et al., 2013).

The Joint Research Centre (JRC) of the EU provides an online tool (the so-called Global Nitrous Oxide Calculator, GNOC) to assess GHG emissions from biofuels in EU legislation (Edwards et al., 2013). This tool calculates N_2O emissions based on the approach of Stehfest and Bouwman (2006). It uses an exponential algorithm that considers site and management specific characteristics such as soil texture, climate, soil organic matter, pH and vegetation. In this model, WOSR was originally in the vegetation class "other" but the JRC recently moved it into the same class as "cereals" without refitting the model (Edwards et al., 2016). This resulted in a calculative reduction of the N_2O emissions from WOSR.

The decision to move WOSR to the cereals group in the GNOC tool is supported by Walter et al. (2015) who used data sets on N_2O emissions from WOSR fields to run a meta-analysis. They also used an exponential model for fertilizer-derived N_2O emission from WOSR, which resulted in even lower N_2O emissions than the GNOC tool.

In regions with strong frost-thaw cycles, high N_2O fluxes can occur during thawing periods (Flessa et al., 1995; Röver et al., 1998). These high thaw pulses can account for more than 50% of the annual N_2O budget from agricultural soils (Kaiser and Ruser, 2001; Jungkunst et al., 2006). Due to these high N_2O winter fluxes, annual measurements are a prerequisite for the reliable quantification of N_2O emissions. Consequently, the duration of the period of trace gas measurements was a criterion for the inclusion (measurements covering > 300 days) or exclusion of data sets in the review by Walter et al. (2015), and only 12 studies with 18 annual datasets (43 data points in total) fulfilled this criterion. Additionally, the small dataset showed a high variability of the N_2O emissions among study sites and also among experimental years.

The main aims of our investigations were therefore: (i) to determine direct annual N_2O emission from WOSR fields over a broad range of production sites, representing areas with a high proportion of WOSR within the crop rotations, thereby extending the currently available data substantially, (ii) to quantify the effect of N fertilization on N_2O fluxes and on yield-related N_2O emission, and (iii) to deduce a fertilizer-related emission factor (FRE) specific for the production of winter WOSR.

2. Materials and methods

2.1. Study sites, experimental design and management

Trace gas measurements were conducted at five study sites located

Table 1
Meteorological, soil chemical and physical characteristics of the study sites.

Study site	Coordinates	MAP 2013/2014/2015	MAT 2013/2014/2015	Soil type (IUSS, 2015[$])	Soil texture[§]			pH[§]	C_{org}[§]	N_t[§]
		[mm a^{-1}]	[°C]		Clay [%]	Silt [%]	Sand [%]	0.01 *M* $CaCl_2$	[%]	[%]
Berge	N 52°37′0″	503	8.7	Luvisol	5.7	19.9	74.4	6.5	1.15	0.09
	E 12°46′60″	615/482/570	9.4/13.0/10.6							
Dedelow	N 53°21′57″	485	8.4	Luvisol	10.0	30.9	59.1	7.4	0.75	0.10
	E 13°49′38″	446/561/414	8.7/9.9/9.7							
Ihinger Hof	N 48°44′41″	688	8.3	Haplic Luvisol	3.2	78.2	18.6	6.8	1.68	0.20
	E 8°55′26″	923/763/544	8.6/10.4/10.1							
Hohenschulen	N 54°18′48″	732	8.9	Haplic Luvisol/Anthrosol	10.5	29.4	60.1	5.9	1.87	0.12
	E 9°59′36″	462/409/562	8.1/9.6/8.8							
Merbitz	N 51°36′58″	520	9.0	Haplic Chernosem	15.8	67.8	16.4	6.6	1.18	0.11
	E 11°91′12″	700/456/429	9.1/10.7/10.4							

MAP: Long-term mean annual precipitation and annual precipitation in the single experimental years; MAT: Long-term mean annual air temperature (2 m) and annual mean air temperature in the single experimental years.
[§] measured in the top soil (0–30 cm).
[$] IUSS Working Group WRB (2015).

in representative areas with a high share of WOSR in the crop rotation. Three sites were located in (1) northern Germany representing approximately 55% of the total German WOSR production area (Hohenschulen, University Kiel; Dedelow, ZALF Müncheberg; Berge, ATB Potsdam-Bornim/Humboldt University Berlin), (2) one site in central Germany (Merbitz, University Halle-Wittenberg) representing 30%, and (3) one site in southern Germany (Ihinger Hof, University Hohenheim) representing 15% of the total German oilseed area. The main characteristics of the study sites are shown in Table 1.

At each site, a randomized split-plot experiment with four replicated blocks was established in 2012. The crop rotation was identical at all sites. All crops of the rotation, winter oilseed rape (var. 'Visby'), winter wheat (var. 'Julius'), and winter barley (*Hordeum vulgare* L., var. 'Tenor' in Berge and var. 'Souleyka' at all other sites), were cultivated as main plots in each of the four blocks. Within the WOSR main plots, at least seven different treatments were included, whereas the main plots with winter wheat and winter barley were managed according to best agricultural management practices without any further differentiation within the crop. Plot size varied slightly over the study sites due to different farming machinery; the minimum size was 3 × 9 m (27 m^2).

WOSR was sown at all sites between end of August and the first two weeks in September (40–45 grains m^{-2}, inter-row width was 0.36 m). In early spring, 90 kg S ha^{-1} were applied as kieserite ($MgSO_4 \cdot H_2O$) to avoid S deficiency in all WOSR treatments including the unfertilized control. After harvest, in the period between mid-July and early August, the soil was ploughed to a depth of 25 cm and winter wheat was subsequently sown at the end of September or in early October. Crop protection and further management measures were conducted according to site-specific agricultural practice. At Berge WOSR straw was removed after harvest whereas it remained on the field at the other study sites. This removed about 20 kg N ha^{-1} a^{-1} (2.8 Mg C ha^{-1} a^{-1}, C/N = 105) from the site Berge (median of all years and treatments).

The treatments of WOSR relevant for results described hereafter, were an unfertilized control and treatments fertilized with 60, 120, 180, or 240 kg N ha^{-1} a^{-1} for yield determination. Typical WOSR fertilization targets in Germany are in the range from 180 kg ha^{-1} a^{-1} to 210 kg ha^{-1} a^{-1}. The 180 kg N ha^{-1} a^{-1} fertilization treatment represents a typical fertilization target value of 200 kg N subtracting N_{min} contents after winter (approximately 20 kg N ha^{-1}). At all sites we measured N_2O fluxes also in additional treatments such as biogas residue application or soil tillage variants. However, these will be discussed in subsequent publications. Trace gas fluxes were measured in every year and at every site in the 120 kg N ha^{-1} and in the 180 kg N ha^{-1} treatment and in some further N treatments (including some of the unfertilized controls) in single years (Table 2). N fertilization to WOSR was split into two equal doses with a first application at the beginning of the growing season and the second application in BBCH-stage 5 (inflorescence emergence, Meier, 2001) approximately four weeks after the first N application. We used calcium ammonium nitrate (CAN) for all N applications.

2.2. Flux measurements

Using the closed chamber method (Hutchinson and Mosier, 1981), flux measurements were conducted at least once a week starting in January or February 2013 and ending in December 2015. Chambers were placed between the seed rows of WOSR, but included the plants for measurements in cereals. In order to place the chambers between the plant rows, the chambers' dimensions were 71 cm length, 27 cm width and 10 cm height. Chamber material was white opaque PVC (PS-plastic, Eching, Germany). They were equipped with rubber sealing, a pressure vent and a ventilator. For measurements, the chambers were anchored on their frames using elastic straps. The frame height was

Table 2
Median of all measured N_2O flux rates as affected by study site, experimental year (Exp. Year) and N fertilization.

Study site	Exp. year	N fertilization [kg N ha^{-1} a^{-1}]			
		0	120	180	240
		N_2O flux [µg N_2O-N m^{-2} h^{-1}]			
Berge	2013	–	2.2	1.3	–
	2014	–	0.7	0.9	–
	2015	–	1.9	1.1	1.3
	2013–2015[$]	–	1.6	1.1	–
Dedelow	2013	–	2.4	2.9	–
	2014	2.2	3.2	3.2	–
	2015	1.9	2.9	2.6	3.0
	2013–2015[$]	–	2.8	2.9	–
Ihinger Hof	2013	–	4.3	8.8	–
	2014	–	5.3	5.3	8.9
	2015	–	1.6	1.7	3.6
	2013–2015[$]	–	3.7	5.3	–
Hohenschulen	2013	2.5	4.8	7.3	–
	2014	3.0	5.2	6.3	–
	2015	–	9.0	8.1	14.2
	2013–2015[$]	–	6.3	7.3	–
Merbitz	2013	6.3	8.7	13.0	–
	2014	4.7	14.2	12.5	–
	2015	3.7	5.9	5.7	7.8
	2013–2015[$]	4.9	9.6	10.4	–

-not determined/not calculated.
[$] Mean values (only given for treatments with 3 years of measurements).

13 cm and they were installed in soil to a depth of 5 to 10 cm. During flux measurements, the chambers were kept closed for one hour; gas samples were taken every 20 min using vacutainers or stopcock vials, resulting in four gas samples per flux measurement. Chamber temperature was recorded for each gas sample. Gas samples were analyzed for N_2O and CO_2 concentrations in the laboratories of the participating research groups by various gas chromatographs equipped with electron capture and flame ionization detectors as well as automatic samplers. Lab inter-comparability was verified by conducting blind inter-comparison measurements between the labs in the beginning of the study. Each laboratory achieved a coefficient of variance below 2% on ten repeated measurements of an ambient N_2O standard gas (data not shown).

2.3. Environmental, soil, and plant analyzes

A climate station was installed next to the experimental plots at each of the study sites. We measured precipitation and air temperature (2 m and 5 cm height). Additionally, soil temperature in one of the four replicated main plots was recorded in 5, 10, and 20 cm soil depth (Logtacs, TRIX-8, CIK solutions, Karlsruhe, Germany).

Simultaneously to each gas sampling, soil samples were taken from 0 to 30 cm depth with an auger. The soil from three insertions per replicate plot was pooled over the four replicates, sieved ($<$ 5 mm) and stored frozen until further analysis. Additionally, in early spring and after harvest of the WOSR N_{min} was determined in 0–30, 30–60, and 60–90 cm depth. These soil samplings were carried out for each plot separately.

For the quantification of mineral N contents, 80 g of soil were extracted with 200 ml of a 0.0125 *M* $CaCl_2$ solution. Concentrations of NO_3^- and NH_4^+ in the extracts were determined using flow-injection analyzers. The analyzers used for that purpose were tested for comparability in an inter-laboratory test. A further aliquot of the soil was used to determine soil moisture by drying at 105 °C for one day.

Before and after soil management events, bulk density of the top soil was determined using stainless steel cylinders (100 ml).

Fresh matter yield was determined by cutting WOSR plants from 1 m^2. The green cut was separated into straw and pods which were flailed subsequently. Moisture was determined after drying for three days at 60 °C. Aliquots of the milled straw and grains were analyzed for C and N using an elemental analyzer (vario Max CN, Elementar Analysensysteme, Hanau, Germany). The oil content of the rapeseeds was determined with NIRS (NIRSystem 5000, Foss, Hamburg, Germany).

2.4. Calculations and statistical analyzes

2.4.1. Flux calculation

Molar gas concentrations were transformed into mass concentrations according to the ideal gas law taking chamber temperature and standard pressure into account. We used several criteria to select the most appropriate flux calculation model and to evaluate the reliability of calculated fluxes. The Akaike information criterion (AIC) was used to decide between flux calculation by the HMR model (Pedersen et al., 2010) and robust linear regression (Huber, 1981). The HMR estimate was used if its AIC value was smaller than the AIC from linear regression and if its kappa value, which controls the curvature, was smaller than 20 h^{-1}. Restricting kappa this way avoids strong overestimation of fluxes due to outliers of the first concentration – time point, which can result in an excellent fit of the nonlinear model but extreme curvatures and flux estimates. A linear regression was applied if only three gas samples were available for flux determination.

The resulting gradients at time zero were multiplied with chamber volume divided by chamber area to derive the flux estimates. For this, the height of the frame was determined after any changes, such as reinstallation after tillage measures. Snow was considered part of the soil and not part of the chamber headspace.

We used the generally clear and significant increase of CO_2 concentration in closed chamber at temperatures above the freezing point to check for accurate diffusive gas accumulation, which can be affected in particular by high wind speed and changing pressure conditions (Hutchinson and Mosier, 1981; Hutchinson and Livingston, 2001). Measured fluxes were subjected to a rigorous quality check since many different people were involved in the comprehensive gas sampling (about 60,000 gas samples were taken in the whole project during the three experimental years) and occasionally different anchoring of the chambers could have resulted in small leakages at the rubber sealing. Thus, the Pearson correlation coefficient between CO_2 concentration and closing time was used as an indicator of the reliability of diffusive gas accumulation. If the Pearson coefficient of the CO_2 flux was smaller than +0.85 and air temperature was above 0 °C, we rated the calculated diffusive flux as considerably biased by other processes and the corresponding flux measurement was excluded from analyses.

Only a few measurements indicated exceptionally high N_2O uptake rates of more than 100 μg N m^{-2} h^{-1}. These fluxes, which were usually associated with abnormally high initial N_2O concentrations, were considered unreliable given that negative diffusion gradients are limited due to low concentration in the atmosphere. Single N_2O flux estimates with extraordinary high uncertainty, i.e., standard errors above 100 μg N m^{-2} h^{-1} (above 25 μg N m^{-2} h^{-1} for uptakes larger than 50 μg N m^{-2} h^{-1}) were also rated as highly unsure and removed. The 90% quantile of all flux standard errors was 11 μg N m^{-2} h^{-1} (median: 1.5 μg N m^{-2} h^{-1}). Thus, the flux detection limit was lower than approximately 2 * SE = 22 μg N m^{-2} h^{-1} for 90% of the flux measurements.

After these rigorous quality checks approximately 10,000 measured N_2O flux rates were analyzed further for the results presented hereafter. Only a very small number of sampling dates were completely lost through the quality check but it resulted in some sampling dates with a reduced number of replicates. Multiple imputation (Honaker et al., 2011) was employed to fill these gaps in plot specific N_2O time series for subsequent statistical analysis. Imputation was done between the replicate N_2O time series group-wise by sites, treatments and years. To improve the performance of imputation, data of each group was transformed as log(flux − min(flux) + 1). The number of multiple imputations was set to 25 and linear time effects were used to account for autocorrelation. The imputed fluxes were then transformed back and cumulated fluxes calculated by linear interpolation. Finally, the median of the multiple imputations was calculated and used as cumulated flux estimate.

2.4.2. Cumulative N_2O emissions and emission factor

For the calculation of annual N_2O emissions we cumulated N_2O fluxes between 1st January and 31st December for each experimental year. We defined this time period at the beginning of our investigations based on the following expectations: except for the sowing, this period covered all soil management and N fertilization measures of WOSR cultivation as well as the time period with presumably increased soil mineral N contents following WOSR harvest and under subsequent winter wheat. Since there was no N fertilization in autumn, we did not expect increased fluxes after rapeseed sowing before winter. Consequently, autumn and early winter fluxes during WOSR cropping were neglected for calculation of annual N_2O emissions.

The FRE was derived by fitting the model described by Walter et al. (2015), which is based on the methodology in Stehfest and Bouwman (2006), after including the data from this study in their dataset (12 sites from the global meta-analysis of Walter et al. (2015) and five sites from this study with three measurement years and up to five fertilization rates per site). Briefly, a linear mixed effects model (R package *lme4* version 1.1–12, Bates et al. (2015), R package *lmerTest* version 2.0-33, Kuznetsova et al. (2016)) relating $\log_{10}$-transformed annual N_2O fluxes to fertilizer N input was fitted. The model included random intercepts

for the site and year effects and a random slope for the year effect. The log_{10}-transformation accounts for the typical higher heterogeneity of larger N_2O fluxes. As a result, the modeled relationship between N_2O fluxes and fertilization rate is exponential and can be compared to previous models by Walter et al. (2015) and Stehfest and Bouwman (2006). Since the model is nonlinear, emission factors depend on the amount of N fertilizer. We report the emission factor for an N fertilization rate of 200 kg N ha^{-1} as this is the amount beyond which no further yield increases are expected under best management practices (Maidl and Limbrunner, 2008). This is also approximately the recommended and typical fertilization rate of WOSR production in Germany. Following the methodology employed by the JRC (Edwards et al., 2016) it was calculated as:

$$EF = \frac{E_{200} - E_0}{200} \quad (1)$$

where E_{200} and E_0 are emissions (kg N_2O-N ha^{-1} a^{-1}) predicted by the model at 200 kg N and 0 kg N fertilization rate, respectively. Compared to the fitted exponential relationship, this linear emission factor approach slightly overestimates emissions from lower N fertilization and underestimates emissions from higher N fertilization. However, these deviations are small as long as the amount of N fertilizer applied does not differ too substantially from typical fertilization rates. In contrast to the IPCC emission factor (EF1) but in accordance with Stehfest and Bouwman (2006), the emission factor takes into account emissions from crop residues indirectly since crop residue N was not included as N input in the model.

2.4.3. Water-filled pore space

Water-filled pore space (WFPS) was calculated as described by Ruser et al. (1998) using the bulk density measured in the top soil of the study sites and assuming a particle density for the soil of 2.65 g cm^{-3}.

2.4.4. N surplus and oil yield-related N_2O emissions

N surplus was calculated by subtraction of N removed from the field by harvest (dry matter concentration of WOSR seed yield multiplied by N concentration of the seeds) from the respective N fertilizer amount. Oil yield–related N_2O emissions for the respective fertilization treatment were calculated by relating annual N_2O emissions to the amount of oil yield, which was the product of WOSR seed yield and oil concentration in the seeds. For the study site Berge, removal of the straw was also taken into consideration.

A linear mixed effects model of log_{10}-transformed oil yield–related N_2O emissions was used to investigate differences between years and N surplus. Year was included as a fixed effect and site as a random intercept.

Finally, total GHG savings of biodiesel produced from the 180 kg N ha^{-1} WOSR treatment were calculated using the Biograce-I (version 4d, www.biograce.net) excel tool.

2.4.5. Statistical analysis

For each site and for each year we separately ran a Kruskal Wallis One Way Anova on Ranks to detect differences between the treatments concerning oil yield-related emissions. Significant differences were determined using a pairwise multiple comparison procedure (Student-Newman-Keuls, $p < 0.05$).

We calculated simple Spearman Rank Order Correlation Coefficients to test for a relationship between the N_2O and CO_2 release in the postharvest period.

All other statistical analyses were conducted using the R language and environment for statistical computing (version 3.3.2, R core, 2016). Mixed-effects models were fitted using package lme4. Confidence intervals of parameters were estimated using parametric bootstrap. Parameter *p*-values were derived using Satterthwaite's approximation for degrees of freedom (Satterthwaite, 1946, R package lmerTest).

Relationships between nitrous oxide fluxes and explaining variables were investigated using Generalized Additive Models (GAM, R package mgcv version 1.8–16, Wood, 2011), which can model non-linear relationships such as the optimum curve typically observed for N_2O emissions vs. soil moisture.

3. Results and discussion

3.1. Meteorological conditions and seasonal N_2O fluxes

3.1.1. Meteorological conditions

Compared to the long-term mean air temperature at every single site, the annual temperature was higher in all experimental years and, except for Hohenschulen, at all study sites (Table 1). Highest annual air temperatures were measured at all sites in the second year of our investigations (2014), followed by the third year (2015). Additionally, considering annual precipitation, which was, depending on site, lowest in the second or third year of measurements, it became obvious that the climatic conditions during our experiment covered a year representing or slightly exceeding long-term conditions (2013), a year with average precipitation and higher temperatures and one year with rather drier and warmer conditions.

3.1.2. N_2O fluxes during the growing season

Spatial and temporal variability of N_2O fluxes was very high (Fig. 1). At all sites, increases of the N_2O fluxes were often detected after N fertilization in conjunction with rainfall events. The highest N_2O flux rate (670 µg N_2O-N m^{-2} h^{-1}) during the whole investigation period in the treatment with 180 kg N ha^{-1} a^{-1} was measured at the Merbitz study site following a heavy rainfall event (42 mm d^{-1}) one week after the second N fertilization in mid May 2013. Prior to this high N_2O pulse, precipitation after two weeks without rainfall had stimulated N_2O release after the first N fertilizer application at the same site.

Although the magnitude of N_2O flux rates differed between study sites and years, we frequently observed short-term N_2O pulses at all study sites after heavy rainfall events throughout the whole growing season as well as after rewetting of solidly dried soil in summer (Fig. 1).

Similar patterns of the N_2O release from arable soils with increased flux rates after N fertilization and rainfall were often reported and explained with enhanced denitrification due to (i) an increased availability of nitrate as substrate for N_2O production, and (ii) due to the formation of anaerobic conditions as a result of lower gas diffusivity in soil water and thus of a reduced O_2 diffusion into the soil combined with O_2 consumption by soil microbes (Flessa et al., 1995; Corre et al., 1996; MacKenzie et al., 1997).

During the first six weeks postharvest we also frequently observed increased N_2O fluxes following rainfall. Monthly fluxes following harvest were often comparable or even exceeding fluxes after N fertilization (Fig. S1). In the post-harvest period we could not see any differentiating effect on the N_2O flux rates, independent of whether the WOSR residues were incorporated into the soil or remained on the surface. Although we did not include WOSR residue incorporation or surface application in our experimental design, we had study sites where we measured increased N_2O fluxes after rainfall when the residues remained on the surface and also after later incorporation (i.e. Dedelow 2014).

Nett et al. (2015) compared the effect of the incorporation of N-rich cauliflower residues on N_2O fluxes with a treatment where the residues remained as mulch on the soil surface. They did not find significant differences of the N_2O release between these two treatments. Baggs et al. (2003) and Escobar et al. (2010) even reported higher fluxes when legume crop residues remained on the soil surface instead of being incorporated.

In this postharvest period after WOSR, nitrate contents in the top soil were generally elevated (Fig. S2). Mosier et al. (1983) reported a threshold of 10 mg nitrate N kg^{-1} soil above which denitrification rates were independent of the soil nitrate concentration. Nitrate-N

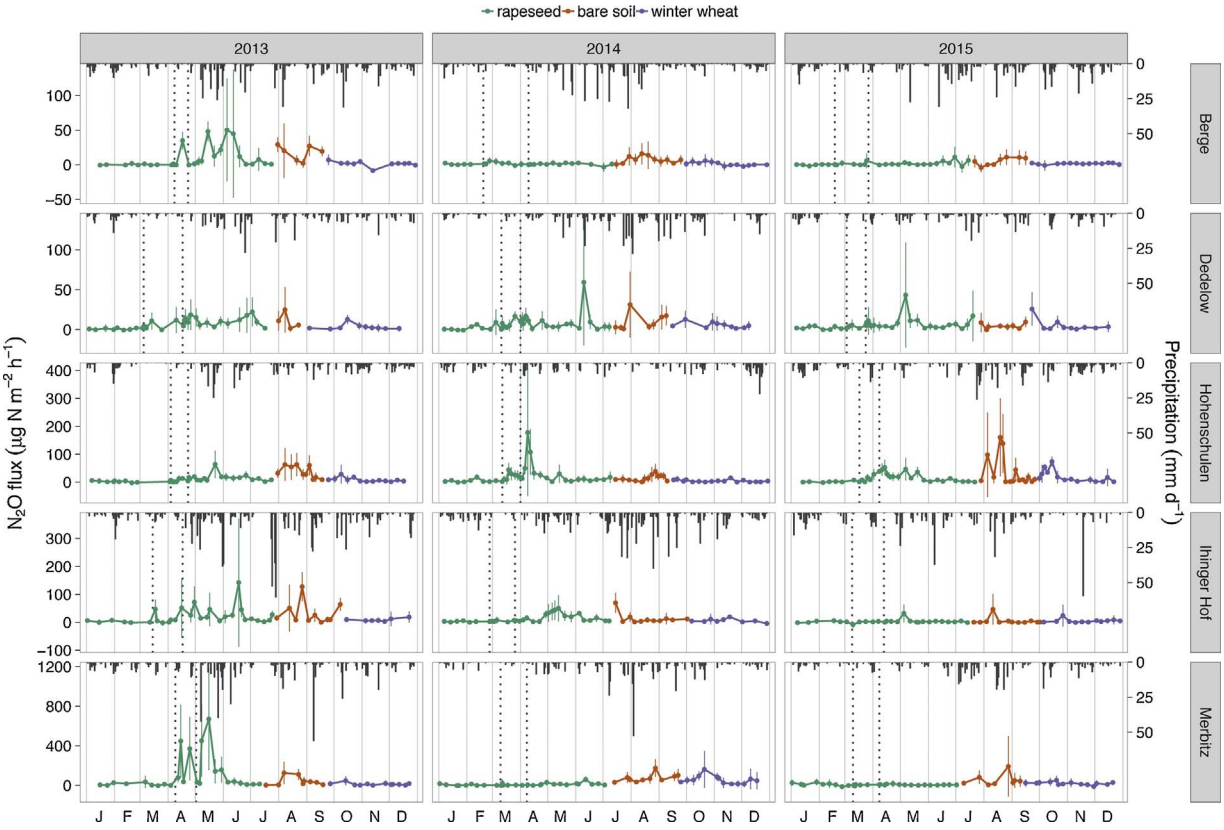

Fig. 1. Mean N_2O flux rate (n = 4) in the treatment with 180 kg N ha^{-1} a^{-1} (colored lines) and daily precipitation (gray bars) as affected by study site and experimental year. Dotted lines represent N fertilization (90 kg N ha^{-1} a^{-1}) each. Note: different y-axis scaling.

concentrations in our study often reached this level immediately after harvest. We therefore concluded that soil nitrate was not a limiting factor for the denitrifying community after harvest and consequently we assume that C availability and corresponding microbial activity and oxygen consumption played a major role as the driver for postharvest N_2O release. This assumption was supported by the statistically highly significant and positive correlations between the N_2O and CO_2 flux rates in the time between harvest of WOSR and seeding of the succeeding winter wheat (Spearman rank correlation coefficients calculated for each study site, all p values were < 0.001, data not shown). It was further supported by the lowest postharvest N_2O flux at the study site Berge, the site with removal of the WOSR straw.

In case of the surface located WOSR residues this C must have been leached from the crop residues during rainfall into the soil or solubilized in regions of the residues with direct soil contact. An alternative explanation could be N_2O production directly from the decomposing plant material (Flessa et al., 2002). Müller et al. (2003) compared the turnover dynamics of different plant residues for modeling purposes. They measured a very low amount of water soluble C in rapeseed straw (~4% of the total C). However, using their algorithm suggested for the relationship between easily available C and the C-to-N ratio we calculated that 36% of the total C in the residues of our treatment with 180 kg N ha^{-1} a^{-1} belonged to the easily decomposable pool.

In contrast to earlier investigations on N_2O fluxes from arable fields or grassland in Germany (Flessa et al., 1995; Kammann et al., 1998; Röver et al., 1998; Kaiser and Ruser, 2000; Ruser et al., 2001), we did not observe considerable N_2O pulses during thawing of frozen soil. We assume that the mild winters in all three experimental years without any severe frost periods were probably the main reason for the low N_2O flux rates observed in our study. It was often shown that frost/thaw induced N_2O pulses increase with increasing duration of frost periods and with severity of the soil freezing (Teepe et al., 2004; Wagner-Riddle et al., 2007; Risk et al., 2013; Xu et al., 2016). Except for the first two weeks of our measurements in 2013, soil temperatures in 10 cm depth did not drop below −2 °C for more than one week at all sites (not shown) and hence the conditions during our field experiment did not enable distinct frost/thaw induced N_2O pulses.

Over the whole data set, we could explain 27% of the variability of the N_2O flux rates (in the treatment with 180 kg N ha^{-1} a^{-1}) with the generalized additive model (Table S1). All smooth terms with a statistically significant contribution to the model results were recorded at the study sites Merbitz, Ihinger Hof, and Hohenschulen, whereas we did not find significant correlations between the smooth terms and the log_{10}-transformed N_2O flux rates at Berge and Dedelow (Fig. S3). We found a relationship between the temperature and soil moisture and the N_2O flux rates for the sites Merbitz, Ihinger Hof, and Hohenschulen. The moisture optimum appeared to be around 50% WFPS. The fluxes at Merbitz were also related to the nitrate contents of the top soil (p < 0.001). Enhanced N_2O flux rates with increasing soil moisture and partly with increasing nitrate contents suggest denitrification as a major source for the N_2O released at the sites Merbitz, Hohenschulen, and Ihinger Hof.

3.2. *Effect of N fertilization on the N_2O fluxes*

Over all sites combined, increasing N fertilization significantly enhanced N_2O flux rates (p < 0.001, Table 3). This effect was more apparent at sites with higher N_2O flux level (Table 2). In contrast, N fertilization effects did not appear at Berge and Dedelow, the sites with the lowest flux levels. Following N fertilization, nitrate and ammonium contents generally increased with increasing N amounts. The increased nitrate contents after N fertilization served as available substrate for N_2O production under conditions supporting denitrification. In contrast, N_2O flux rates were negligible under conditions favorable for nitrification (high ammonium concentrations and soil moisture contents below field capacity).

Table 3
Best linear mixed effects model for rapeseed-specific annual N_2O emissions (N_2O_{annual} in kg N ha^{-1} a^{-1}) for the data in this study pooled with the data from Walter et al. (2015); the variance explained by the random effects, the residual variance and R^2 values are given. R^2 values describe correlation between annual fluxes and predicted (from the fixed effects only and from the complete model) values on the natural scale.

Log_{10} (flux mean) = a + b N_{amount}				
Back transformed to natural scale Flux mean = 10^a $10^{(b \times Namount)}$		Coefficients and 95% confidence intervals in brackets	a = −0.169 (−0.406, −0.068) b = 0.00222 (0.0011, 0.0033)	
Random effects			R^2	
On intercept (variance)	On slope (variance)	Residual variance	fixed effects only	complete model
Site, year (0.100, 0.063)	Year 2e-6	0.021	0.05	0.88

Several field experiments showed positive correlations between the N_2O flux rates and soil nitrate contents (Ruser et al., 2001; Sehy et al., 2003; Jones et al., 2007). Especially for agricultural soils, it was also reported that increased nitrate availability can inhibit the N_2O reductase activity due to the competitive effect of nitrate and N_2O as terminal electron acceptors during denitrification thus stimulating N_2O release from denitrification (Cho and Sakdinan, 1978; Blackmer and Bremner, 1978).

3.3. Effect of study site on the N_2O fluxes

The study site had a significant and strong effect on the N_2O flux rates ($p < 0.001$, Table 3). The median N_2O flux rate over the entire three experimental years in the treatment with a N fertilizer amount of 180 kg N ha^{-1} a^{-1} decreased in the order Merbitz (10.4 µg N_2O-N m^{-2} h^{-1}) > Hohenschulen (7.3 µg N) > Ihinger Hof (5.3 µg N) > Dedelow (2.9 µg N) > Berge (1.1 µg N) (Table 2).

Merbitz, the site with the highest clay content, exhibited the highest flux rates, particularly in the first experimental year (Fig. 1, Table 2). At the sites at Berge and Dedelow, we generally measured low N_2O flux rates. Except for Dedelow in July 2014, N_2O fluxes at these two sites did not exceed 25 µg N_2O-N m^{-2} h^{-1} during the entire experimental period (Fig. 1). These low fluxes were probably a result of the sandy soil texture (Table 1) and the corresponding low water holding capacity enabling good soil aeration. These results are in agreement with N_2O flux measurements in wheat fields on soils differing strongly in soil texture. Pelster et al. (2012) reported annual N_2O emissions between 0.6 and 0.7 kg N_2O-N ha^{-1} from a sandy soil under wheat fertilized with calcareous ammonium nitrate and between 5.1 and 8.3 kg N_2O-N ha^{-1} from a silty clay soil under the same management. In a lysimeter study with three differently textured soils (clay loam, loam, sand) Jamali et al. (2016) reported decreasing N_2O fluxes with increasing portions of sand. They attributed low N_2O fluxes from sandy soils to a lower N_2O production from denitrification, since a higher proportion of macro-pores responsible for drainage and aeration in sandy soils reduces the frequency of conditions favoring denitrification.

Although soil texture at the site Hohenschulen is also sand-dominated (Table 1), N_2O fluxes measured there were distinctively higher than at the sandy sites at Dedelow and Berge (Table 2). Especially for sandy soils, Pelster et al. (2012) assumed a temporal C limitation for denitrifying microorganisms requiring C compounds as electron donator. An increase in the C_{org} content of the soil therefore also enhances the availability of C for the denitrifying microbial community. Stehfest and Bouwman (2006) in their analysis of N_2O emission data from 1008 agricultural soils confirmed the effect of rising N_2O emissions with increasing C_{org} content of topsoil.

The C_{org} content of the topsoil in Hohenschulen was 1.6 and 2.5 times higher than in Berge and Dedelow, respectively (Table 1). For the period between 1st January and the sowing of wheat in autumn of the first experimental year, our flux chambers covered bare soil. The CO_2 flux rates (which are only a rough estimate due to the chamber closing times being optimized for N_2O flux measurements) are therefore an indicator for C mineralization. The mean CO_2 flux rate at Hohenschulen in that period was 86.9 mg CO_2-C m^{-2} h^{-1}. It was 1.6 and 2.3 times higher than the corresponding mean flux rates at Berge and Dedelow. We therefore presume that the higher soil respiration rates at Hohenschulen decreased O_2 availability, thus favoring anaerobic conditions and N_2O production during denitrification whereas O_2 supply in the soils in Berge and Dedelow was sufficient to impede nitrate reduction. This would explain the higher N_2O fluxes compared to the other sandy sites (Table 2).

3.4. Inter-annual variability of the N_2O fluxes

The median annual N_2O flux at all sites exhibited a high variability and the effect of the experimental years was statistically significant and of the same order of magnitude as the site effect (Table 3). The highest inter-annual variability was measured at the study site Ihinger Hof in the treatment with 180 kg N ha^{-1} a^{-1}. At this site, the flux was 5 times higher in 2013 than in 2015 (Table 2).

A main driver for the inter-annual variability of the annual N_2O flux rates was rainfall shortly after N fertilization or harvest. In the treatment with 180 kg N ha^{-1} a^{-1}, the annual N_2O flux rate decreased at all experimental sites in the same order as the annual precipitation decreased (Fig. 2). This clearly indicates that local weather conditions and in particular the amount of rainfall (especially in months with increased mineral N availability as, for example after N fertilization; Fig. S2), play a key role in determining the magnitude of N_2O flux rates.

A high inter-annual variability of N_2O fluxes has often been reported in field studies with N_2O measurements (Dobbie et al., 1999; Pfab et al., 2011; Reeves and Wang, 2015) as well as in modeling approaches from sites with different climate conditions (Leip et al., 2011) or with different climate scenarios (Ben Aoun et al., 2016). Despite a uniform management (N fertilization, crop type) annual N_2O emission varied by up to factor seven between the single experimental years. These differences also resulted from different weather conditions during the study, with rainfall being one of the dominant drivers for N_2O release from soils (Smith et al., 1998; Dobbie et al., 1999; Laville et al., 2011).

3.5. Cumulative N_2O emissions and fertilizer-related N_2O emissions

Due to high variability of N_2O fluxes, cumulative N_2O emissions were also scattered widely over the study sites and experimental years. For the treatment fertilized with 180 kg N ha^{-1} a^{-1}, annual N_2O emission varied between 0.24 kg N_2O-N ha^{-1} a^{-1} (Berge, 2014) and 5.48 kg N_2O-N ha^{-1} a^{-1} (Merbitz, 2013) (Fig. 3).

The magnitude of annual N_2O emissions was in the same range as those assembled by Walter et al. (2015) in their meta-analysis on the effect of N fertilization on N_2O emissions from WOSR fields. For N fertilizer amounts approximately in the same range as our 180 kg N ha^{-1} a^{-1} treatment Walter et al. (2015) reported annual N_2O emissions from WOSR fields ranging between 0.31 and 5.61 kg N_2O-N ha^{-1} a^{-1}.

Since N_2O flux rates were stimulated with increasing N fertilizer amount, cumulative N_2O emissions also increased with N fertilization (Fig. 3). We supplemented the dataset of Walter et al. (2015) with our data, thereby doubling the number of data points, and following their methodology, derived an exponential model relating N_2O emissions to N fertilization (Table 3). The model confirmed a strong impact of study sites and years on annual N_2O fluxes. A nonlinear response of N_2O emissions to N fertilization has often been reported and explained either with an increased N supply strongly exceeding N demand of the crop or with extended periods of increased mineral N supply for N_2O

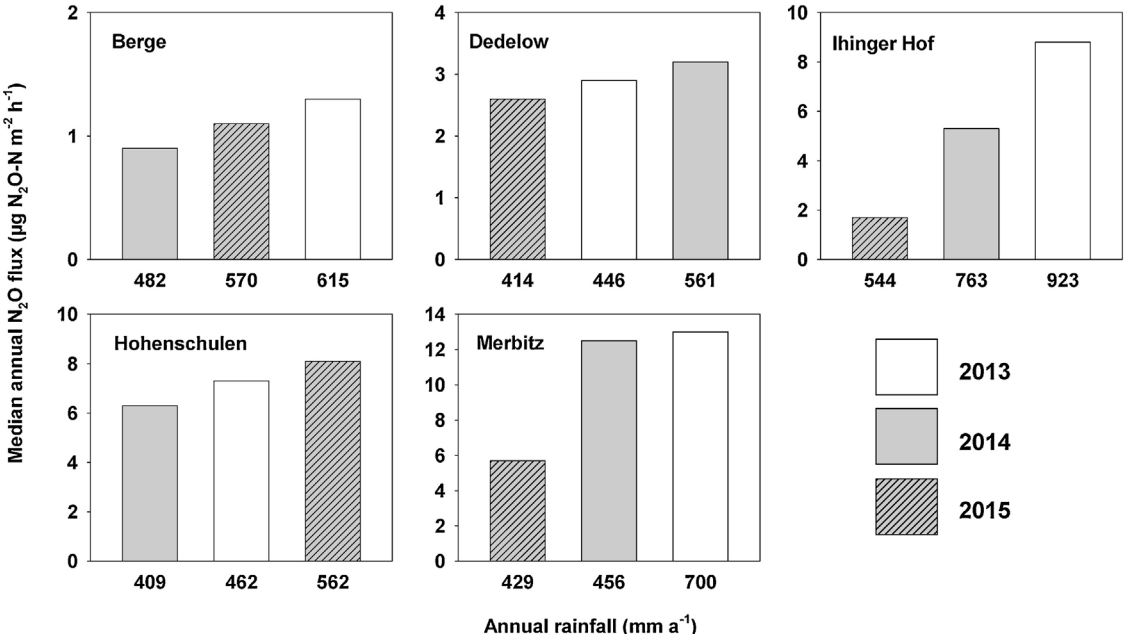

Fig. 2. Median N_2O flux and annual precipitation at the five study sites. Note: different y-axis scaling and non-equidistant x-axis units.

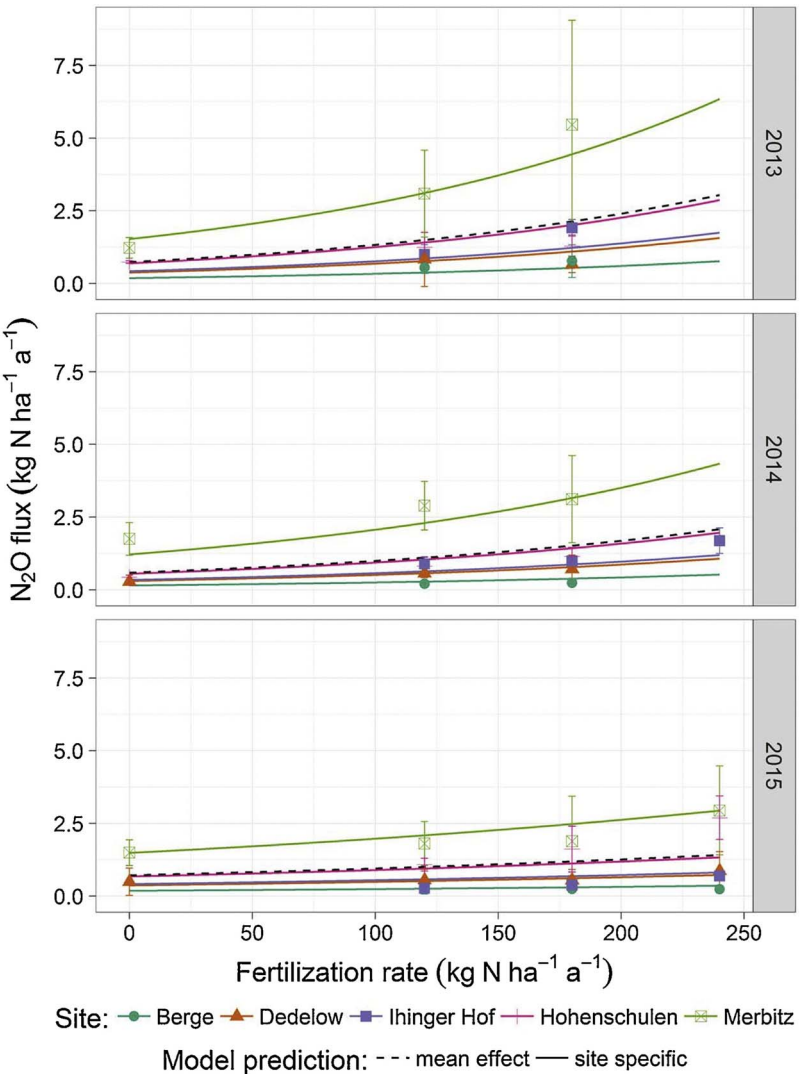

Fig. 3. Mean measured cumulative annual N_2O emission (n = 4, ± standard deviation) at different nitrogen fertilization rates. Lines depict site-specific and mean N_2O emissions modeled with the mixed effects model described in Table 3.

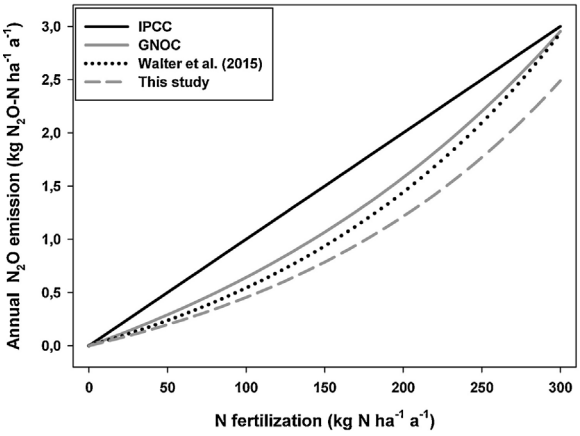

Fig. 4. Effect of different fertilizer-related N_2O emission models on the calculative fertilizer-derived N_2O emission from WOSR fields as affected by N fertilizer amount. IPCC assumes a linear increase of N_2O emission with N application rate (constant emission factor of 1%), GNOC (Edwards et al., 2016), Walter et al. (2015) and the model derived in this study describe fertilizer-derived N_2O emissions as an exponential function of fertilizer N input. The GNOC line represents rapeseed at temperate oceanic sites with 1–3% SOC, pH 5.5–7.3, and medium soil texture.

Table 4
Mean oil yield [Mg ha^{-1} a^{-1}] as affected by study site, N fertilization and experimental year. Different letters indicate statistically significant differences between the N-fertilizer treatments within one year and one study site (Student-Newman-Keuls Method, $p < 0.05$).

Study site	Year	N fertilization				
		kg N ha^{-1} a^{-1}				
		0	60	120	180	240
Berge	2013	1.17 ^{b}	1.29 ^{a,b}	1.38 ^{a,b}	1.38 ^{a,b}	1.72 ^{a}
	2014	1.63 ^{c}	1.92 ^{b,c}	2.28 ^{a,b}	2.42 ^{a}	2.56 ^{a}
	2015	0.97 ^{c}	1.50 ^{b}	1.74 ^{a}	1.87 ^{a}	1.85 ^{a}
	Mean	1.26	1.57	1.80	1.89	2.04
Dedelow	2013	2.36 ^{b}	2.62 ^{a}	2.73 ^{a}	2.79 ^{a}	2.78 ^{a}
	2014	2.43 ^{a}	2.56 ^{a}	2.67 ^{a}	2.74 ^{a}	2.71 ^{a}
	2015	1.97 ^{a}	2.09 ^{a}	2.10 ^{a}	2.05 ^{a}	2.13 ^{a}
	Mean	2.25	2.42	2.50	2.53	2.54
Ihinger Hof	2013	1.59 ^{b}	1.78 ^{a}	2.01 ^{a}	1.96 ^{a}	1.92 ^{a}
	2014	1.22 ^{c}	1.52 ^{b}	1.76 ^{a,b}	1.83 ^{a}	1.91 ^{a}
	2015	1.55 ^{c}	1.64 ^{b,c}	1.76 ^{a,b}	1.86 ^{a}	1.88 ^{a}
	Mean	1.45	1.65	1.84	1.88	1.90
Hohenschulen	2013	1.64 ^{b}	2.01 ^{a}	2.25 ^{a}	2.32 ^{a}	2.40 ^{a}
	2014	2.02 ^{a}	2.35 ^{a}	2.50 ^{a}	2.55 ^{a}	2.60 ^{a}
	2015	1.78 ^{c}	2.04 ^{a,b}	2.21 ^{a}	1.99 ^{b}	2.15 ^{a,b}
	Mean	1.81	2.13	2.32	2.29	2.38
Merbitz	2013	1.61 ^{b}	1.75 ^{a,b}	1.87 ^{a,b}	1.88 ^{a,b}	1.96 ^{a}
	2014	1.18 ^{d}	1.61 ^{c}	2.09 ^{b}	2.23 ^{b}	2.38 ^{a}
	2015	1.11 ^{b}	1.30 ^{b}	1.67 ^{a}	1.78 ^{a}	1.64 ^{a}
	Mean	1.30	1.55	1.88	1.96	2.00

production (van Groeningen et al., 2010; Hoben et al., 2011; Shcherbak et al., 2014).

The German legislation on N fertilization (DüV, 2006) currently allows for an N surplus (N fertilization minus N removal with harvest) of 60 kg N ha^{-1} a^{-1} (mean value of three years). Assuming a high WOSR yield of 5 Mg ha^{-1} a^{-1} we can deduce a crop demand of 227 kg N ha^{-1} a^{-1} (5 Mg ha^{-1} a^{-1} × 45.4 kg N Mg^{-1}, cf. Table 1 of DüV, 2006). On a legislative basis, it can therefore be expected, that N fertilization in German WOSR production potentially varies between 0 and 287 kg N ha^{-1}. Over this range of N fertilization, all proposed nonlinear models for the N_2O emission – N fertilization rate relationship (Fig. 4) result in lower fertilizer-related N_2O emissions when compared to the linear IPCC Tier 1 approach.

Comparing the impact of different emission factors for direct N_2O field emissions from WOSR cultivation in Poland, Syp et al. (2016) also reported higher N_2O emission calculated with the BioGrace approach (IPCC default values, Tier 1) compared to the GNOC.

Assuming a fertilizer amount of 200 kg N ha^{-1} a^{-1} the global FRE factor derived from the exponential model was 0.6% (CI: 0.31%–1.00%). This factor is within the uncertainty range of the EF1 IPCC emission factor (0.3%–3%), but about 40% lower than the IPCC default value and was also lower than the FRE calculated by GNOC and by Walter et al. (2015) (Fig. 4).

One reason for the lower FRE in our experiment may be the fact that two of our five study sites have sandy, well aerated soils with low C_{org} contents. These were chosen because they are representative for a large part of the German WOSR production area.

A second reason might be the absence of distinct frost/thaw cycles at all study sites. As a consequence, the absence of frost/thaw cycles results in N_2O emissions about half as high as in case of frost/thaw cycle occurrence. However, such mild winters with less frost/thaw cycles seem to have become more frequent in Germany as a result of ongoing climate change (Kreyling and Henry, 2011).

The low rapeseed FRE factor is in good agreement with results from recent studies in the UK which also observed lower FRE factors than the IPCC default (Bell et al., 2015). Based on multiple field experiments with different crops including WOSR a new national emission factor of 0.46% was derived for the UK (Sylvester-Bradley et al., 2015). Similarly, a recent multi-site study in France, again including WOSR in the field experiments, observed lower N_2O emissions than expected from the IPCC default emission factor (Le Gall et al., 2014).

3.6. Oil yield and yield-related N_2O emissions

The highest mean seed yields over all three experimental years were achieved in Dedelow (5.38 Mg ha^{-1} a^{-1}) and in Hohenschulen (4.67 Mg ha^{-1} a^{-1}). At the remaining three sites (Berge, Merbitz and Ihinger Hof) seed yield was lower and ranged between 3.97 and 4.22 Mg ha^{-1} a^{-1}. The mean seed yields over all sites were 4.54, 4.90,

Table 5
Mean oil yield-related N_2O emission [kg N_2O-N Mg^{-1} oil ha^{-1}] as affected by study site, N fertilization and experimental year. Different letters indicate statistically significant differences between the N fertilizer treatments within one year and one study site (Student-Newman-Keuls Method used for comparison of three or more treatments, *t*-test for comparison of two treatments, $p < 0.05$).

Study site	Year	N fertilization			
		kg N ha^{-1} a^{-1}			
		0	120	180	240
Berge	2013	–	0.50 ^{a}	0.58 ^{a}	–
	2014	–	0.07 ^{a}	0.10 ^{a}	–
	2015	–	0.31 ^{a}	0.15 ^{a}	0.14 ^{a}
	Mean$^{\$}$	–	0.29	0.28	–
Dedelow	2013	–	0.18 ^{a}	0.24 ^{a}	–
	2014	0.13^{a}	0.23 ^{a}	0.26 ^{a}	–
	2015	0.25^{a}	0.27 ^{a}	0.30 ^{a}	0.35 ^{a}
	Mean$^{\$}$	–	0.23	0.27	–
Ihinger Hof	2013	–	0.53 ^{b}	0.97 ^{a}	–
	2014	–	0.56 ^{a}	0.52 ^{a}	0.99 ^{a}
	2015	–	0.19 ^{b}	0.19 ^{b}	0.41 ^{a}
	Mean$^{\$}$	–	0.42	0.56	–
Hohenschulen	2013	0.51 ^{a}	0.58 ^{a}	0.55 ^{a}	–
	2014	0.21 ^{b}	0.31 ^{b}	0.47 ^{a}	–
	2015	–	0.54 ^{b}	0.85 ^{a,b}	1.52 ^{a}
	Mean$^{\$}$	–	0.49	0.56	–
Merbitz	2013	0.75^{a}	1.59 ^{a}	2.98 ^{a}	–
	2014	1.48 ^{a}	1.45 ^{a}	1.36 ^{a}	–
	2015	1.43^{a}	1.03 ^{a}	1.12 ^{a}	1.93 ^{a}
	Mean$^{\$}$	1.22	1.36	1.82	–

– not determined/not calculated.
$^{\$}$ Mean values were only calculated for treatments with 3 years measurements.

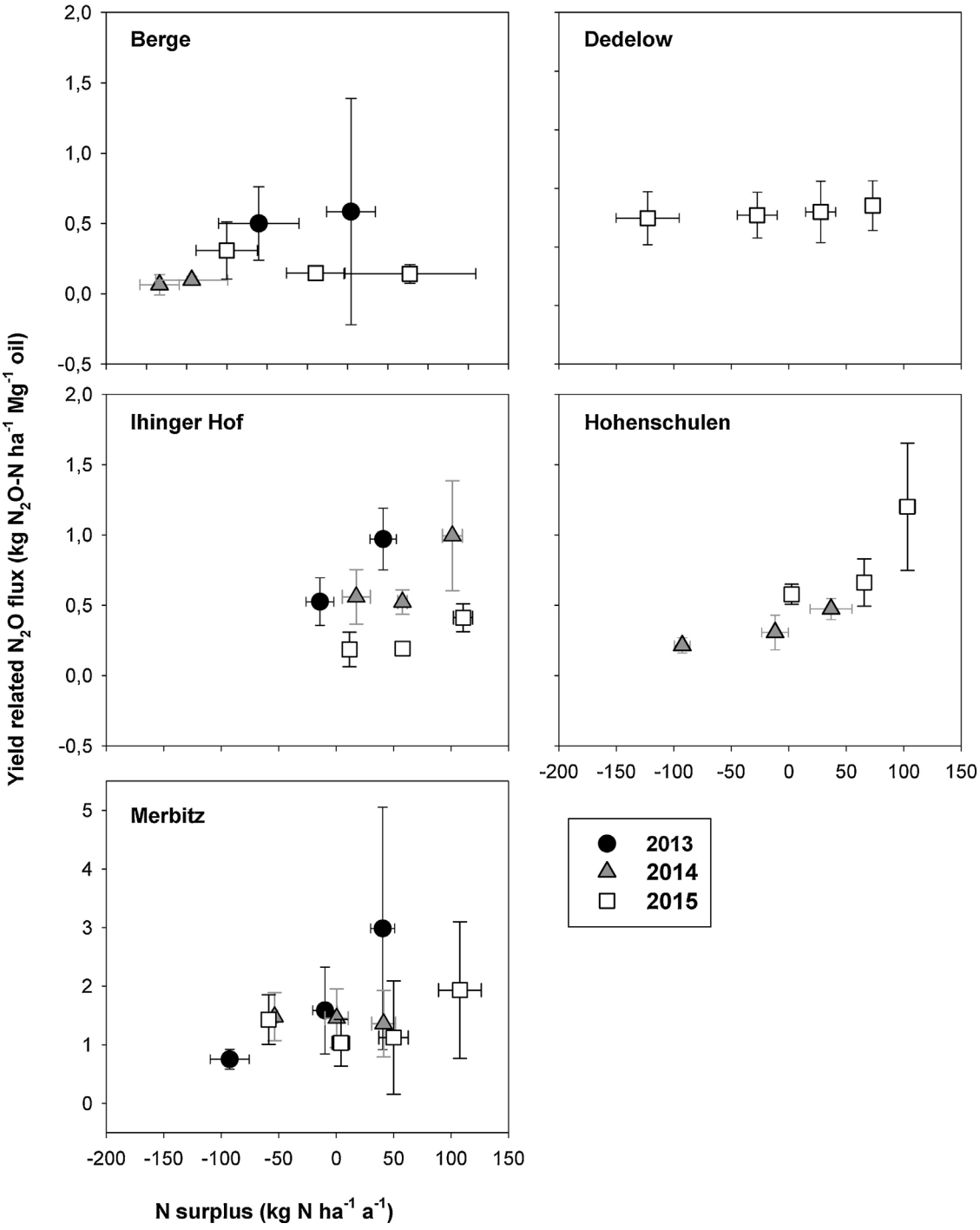

Fig. 5. Relationship between mean N surplus and mean oil yield-related N_2O emission (n = 4, ± standard deviation) as affected by study site and experimental year. At the site Berge straw removal was also taken into consideration for the calculation of the N surplus. Note: different y-axis scaling.

and 4.03 Mg ha^{-1} a^{-1} in 2013, 2014, and 2015, respectively. These yields follow the pattern of mean German WOSR yields, which were 3.96, 4.48, and 3.91 Mg ha^{-1} a^{-1} in 2013, 2014, and 2015, respectively (German Federal Statistical Office, 2017). Research studies commonly achieve better yields than commercial farms, but the identical annual pattern emphasizes the representativeness of our compilation of study sites for German WOSR production.

The reason for the high yield at Dedelow remains unclear. A possible explanation is a pool of easily mineralizable N, resulting from long-term application of organic fertilizers to silage maize and sugar beet approximately every second year before our experiment. However, C_{org} and total N contents at this site were comparatively low. Unfortunately, we did not determine N contents of the WOSR seeds in every year and at every site since we focused on oil yield as the relevant target yield. However, for the year 2015 we determined an N uptake in the seeds of 123 kg N ha^{-1} in the unfertilized treatment at Dedelow. The only study site with N uptake measurements in the unfertilized treatment in the same year was Merbitz with 59 kg N ha^{-1}. Further N uptake data for unfertilized treatments at other sites than Dedelow in 2013 and 2014 varied between 54 and 93 kg N ha^{-1}. The high N uptake in the rapeseeds at Dedelow was not only a result of increased biomass growth but also enhanced N concentrations (not shown). Both, high biomass and N concentration in the seed of the unfertilized treatment in Dedelow indicates a high and easily available N delivery at

Table 6
GHG emissions and savings of biofuel produced from the 180 kg N ha^{-1} a^{-1} treatment according to BioGrace-I GHG calculation tool (version 4d). Standard values were used for all values not given in the Table.

Mineral N fertilizer	kg N ha^{-1} a^{-1}	180	180	180	180	180	180
Production of N fertilizer	g CO_2-eq kg^{-1}	3652[1]	3652[1]	3652[1]	3652[1]	3652[1]	3652[1]
Emission factor for direct N_2O field emissions from mineral fertilizer N	%	1	1	0.6	0.6	0.6	0.6
Emission factor for direct N_2O field emissions from crop residues (IPCC default)	%	1	1	1	1	0.6	0.6
Fresh matter seed yield	Mg ha^{-1} a^{-1}	4.99	4.99	4.99	4.99	4.99	4.99
Soil water saturation high?		yes[2]	yes[2]	yes[2]	yes[2]	yes[2]	yes[2]
Direct and indirect N_2O field emissions	kg N_2O ha^{-1} a^{-1}	5.87	5.87	4.77	4.77	4.09	4.09
	kg N_2O-N ha^{-1} a^{-1}	3.74	3.74	3.04	3.04	2.60	2.60
Fossil fuel reference	g CO_2-eq MJ^{-1}	83.8	95.1[3]	83.8	95.1[3]	83.8	95.1[3]
GHG emission reduction vs reference	%	44	51	47	54	50	56

[1] Biograce standard emission factor for CAN.
[2] This setting accounts for 30% loss of input N via nitrate leaching. The alternative is zero nitrate leaching.
[3] New reference value (fossil diesel) according to EU directive 2015/1513 (EU, 2015).

this site.

The median flux over all sites and years in the treatment with 180 kg N ha^{-1} a^{-1} related to grain yield was 0.22 kg N_2O-N Mg^{-1} oilseed grain.

Oil yield varied between 0.97 and 2.79 Mg ha^{-1} a^{-1} (Table 4), the median oil yield was 2.00 Mg ha^{-1} a^{-1}. Due to the high seed yield, oil yield was also highest at study site Dedelow, where 2.25 Mg ha^{-1} a^{-1} was achieved even in the unfertilized treatment. With few exceptions (Hohenschulen 2015 and Merbitz 2014) N fertilization higher than 120 kg N ha^{-1} did not result in statistically significant increases in oil yield.

This result is in agreement with Hegewald et al. (2016) who reported only small increases in oil yield (0.04 Mg ha^{-1} a^{-1}) when N fertilization was increased from 120 to 180 kg N ha^{-1} a^{-1} in a study on the effect of different preceding crops on WOSR yield. As mentioned by Rathke et al. (2006) N fertilization increases the crude protein content of rapeseeds at the expense of oil concentration. We also observed declining oil contents with increasing N fertilization, however, due to higher dry matter development with increasing N supply, oil yields were stable over the N fertilizer range between 120 and 240 kg N ha^{-1} a^{-1} (Table 4).

Oil yield–related N_2O emissions varied depending on site and year. The median yield-related N_2O emission over the entire data set was 0.46 kg N_2O-N Mg^{-1} oil. Cumulative annual N_2O emissions, and consequently oil yield-related N_2O emissions, were lowest at study sites Berge and Dedelow (Table 5). For 2014 and 2015 we found a tendency at Dedelow for increasing yield-related emission with increasing N fertilization.

In contrast, oil-yield related N_2O emissions were distinctly higher in all years for the site Merbitz with its silty Chernozem soil and also higher for the sites Ihinger Hof and Hohenschulen (Table 5). Increasing N fertilization at these three sites by 60 kg N ha^{-1} from 120 to 180 kg N ha^{-1} a^{-1} resulted in a slight increase (approximately 0.15 kg N_2O-N Mg^{-1}) in yield-related N_2O emissions whereas the application of another 60 kg N ha^{-1} a^{-1} (in total 240 kg N ha^{-1} a^{-1}) approximately doubled the yield-related emissions in the respective years with trace gas measurements indicating a threshold for strongly enhanced yield-related N_2O emissions between fertilization intensities of 180 and 240 kg N ha^{-1} a^{-1}.

Different functions have been used to visualize the relation of yield-related N_2O emissions to N surplus. Van Groenigen et al. (2010) used an exponential function to describe the yield-related N_2O emissions with N surplus in silage maize. Walter et al. (2015) fitted a segmented linear function to their WOSR yield dry mass-related N_2O emissions and found a critical N surplus of 80 kg N ha^{-1} where the yield-related N_2O emissions substantially increased. We found neither a clear threshold in our experiment nor a simple global relationship. This can be attributed to the high inter-annual variability of the N_2O emissions (Fig. 5). Especially in 2013, N_2O emissions were driven by fertilization whereas emissions in 2014 and 2015 did depend less on fertilization and were generally lower. Oil yield-related N_2O emissions at the study sites Ihinger Hof and Merbitz increased with a small N surplus in 2013, the year with the highest precipitation, whereas the threshold for increased yield-related N_2O emissions under drier conditions in 2014 and 2015 was approximately +50 kg N ha^{-1} N surplus. The site Hohenschulen also exhibited a distinct increase of yield-related N_2O emission with rising N surplus, whereas the low emission sites Berge and Dedelow did not respond to varying N surpluses. The removal of WOSR straw at the site Berge resulting in lower N surplus values might have additionally affected N_2O emissions.

Calculating the GHG balance of biodiesel produced from the 180 kg N ha^{-1} a^{-1} WOSR treatment according to current EU RED methodology (i.e., using the IPCC emission factor of 1%) resulted in GHG savings of 44% and 51% compared to the current and updated fossil fuel reference, respectively (Table 6). Note that both yield (4990 kg ha^{-1} a^{-1}) and N fertilization of the 180 kg N treatment were much higher than the EU RED default values (3113 kg ha^{-1} a^{-1} with 137.4 kg N fertilization). Substituting the EF1 IPCC emissions factor with the rapeseed specific emissions factor of 0.6% for the calculation of direct N_2O field emissions from fertilizer N input improved GHG savings to 47% and 54%, respectively. If we assume that the same WOSR-specific emission factor is also valid for emissions from the crop residues, GHG savings even achieve 50% and 56%, respectively. Thus, a full update of the emission factor results in a calculative increase of GHG savings by five to six percentage points. As a result the 50% goal of the EU RED would be achieved even with the original reference value.

4. Conclusions

With our study covering three years at five study sites in representative regions of German WOSR production, we doubled the experimental base (now 86 annual flux values) for the deduction of an emission factor for fertilizer-related N_2O emissions from WOSR cropping. Our measurements confirmed the result of Walter et al. (2015) that fertilizer-related N_2O emissions from WOSR are markedly lower than the (linear) one percent default value proposed by the IPCC Tier 1 approach. For a common N fertilizer amount of 200 kg N ha^{-1} a^{-1} in German WOSR cultivation the fertilizer-related emission factor developed from our data set combined with the data assembled by Walter et al. (2015) is 0.6%. Applying this WOSR-specific emission factor to the N fertilizer amount used in our experiment (180 kg N ha^{-1} a^{-1}), which is similar to the amounts used under best agricultural management conditions, we could show, that the GHG reduction criteria stipulated by the Renewable Energy Directive for biofuels can be fulfilled for existing biofuel plants: the GHG emissions from biofuel production achieved more than 50% GHG savings compared to fossil diesel exploration and consumption, especially if best management practices are adopted in WOSR cultivation.

Our oil yield results indicate that there is potential for reduction of N fertilization in comparison to agricultural practice recommendations

without oil yield losses. This would be an excellent mitigation option due to avoiding GHG emissions during fertilizer production and the reduction of direct and indirect N_2O field emissions.

Acknowledgements

The project would not have been possible without the diligent work of technical staff and students, for which we are very grateful.

The study was funded by the German Federal Ministry of Food and Agriculture and managed by the Agency for Renewable Resources under grants 22403212, 22403312, 22403412, 22403512, 22403712, 22403812, and 22403912. We also acknowledge the financial support of the Union for the Promotion of Oil and Protein Plants, Germany.

Appendix A. Supplementary data

Supplementary data associated with this article can be found, in the online version, at http://dx.doi.org/10.1016/j.agee.2017.07.039.

References

Baggs, E.M., Stevenson, M., Pihlatie, M., Regar, A., Cook, H., Cadisch, G., 2003. Nitrous oxide emissions following application of residues and fertilizer under zero and conventional tillage. Plant Soil 254, 361–370.

Bates, D., Maechler, M., Bolker, B., Walker, S., 2015. Fitting linear mixed-effects models using lme4. J. Stat. Softw. 67, 1–48.

Bell, M.N., Hinton, N., Cloy, J.M., Topp, C.F.E., Rees, R.M., Cardenas, L., Scott, T., Webster, C., Ashton, R.W., Whitmore, A.P., Balshaw, H., Paine, F., Goulding, K.W.T., Chadwick, D.R., 2015. Nitrous oxide emissions from UK arable soils Fluxes, emission factors and mitigation. Agric. Ecosyst. Environ. 212, 134–147.

Ben Aoun, W., El Akkari, M., Flénet, F., Jacquet, F., Benoit, G., 2016. Recommended fertilization practices improve the environmental performance of biodiesel from winter oilseed rape in France. J. Clean. Prod. 139, 242–249.

Blackmer, A.M., Bremner, J.M., 1978. Inhibitory effect of nitrate on reduction of N_2O to N_2 by soil microorganisms. Soil Biol. Biochem. 10, 187–191.

Bouwman, A.F., 1996. Direct emission of nitrous oxide from agricultural soils. Nutr. Cycl. Agroecosyst. 46, 53–70.

Bremner, J.M., 1997. Sources of nitrous oxide in soils. Nutr. Cycl. Agroecosyst. 49, 7–16.

Butterbach-Bahl, K., Baggs, E.M., Dannenmann, M., Kiese, R., Zechmeister-Boltenstern, S., 2013. Nitrous oxide emissions from soils: how well do we understand the processes and their controls? Phil. Trans. R. Soc. B: Biol. Sci. 368.

Carré, P., Pouzet, A., 2014. Rapeseed market, worldwide and in Europe. OCL 21, D102.

Cho, C.M., Sakdinan, L., 1978. Mass spectrometric investigation on denitrification. Can. J. Soil Sci. 58, 443–457.

Clais, P., Sabine, C., Bala, G., Bopp, L., Brovkin, V., Canadell, J., Chhabra, A., DeFries, R., Galloway, J., Heimann, M., Jones, C., Le Quéré, C., Myneni, R.B., Piao, S., Thornton, P., 2013. Carbon and other biogeochemical cycles. In: Stocker, T.F., Qin, D., Plattner, G.-K., Tignor, M., Allen, S.K., Boschung, J., Nauels, A., Xia, Y., Bex, V., Midgley, P.M. (Eds.), Climate Change 2013: The Physical Science Basis Contribution of Working Group I to the Fifth Assessment Report of the Intergovernmental Panel on Climate Change. Cambridge University Press Cambridge, United Kingdom and New York, NY USA, pp. 465–570.

Corre, M.D., Van Kessel, C., Pennock, D.J., 1996. Landscape and seasonal patterns of nitrous oxide emissions in a semiarid region. Soil Sci. Soc. Am. J. 60, 1806–1815.

Crutzen, P.J., Mosier, A.R., Smith, K.A., Winiwarter, W., 2008. N_2O release from agro-biofuel production negates global warming reduction by replacing fossil fuels. Atmos. Chem. Phys. 8, 389–395.

Crutzen, P.J., 1981. Atmospheric chemical processes of the oxides of nitrogen including nitrous oxide. In: Delwiche, C.C. (Ed.), Denitrification, Nitrification and Atmospheric N_2O. Wiley, Chichester, pp. 17–44.

Dobbie, K.E., McTaggart, I.P., Smith, K.A., 1999. Nitrous oxide emissions from intensive agricultural systems: variations between crops and seasons; key variables; and mean emission factors. J. Geophys. Res. 104, 26891–26900.

Dufossé, K., Gabrielle, B., Drouet, J.-L., Bessou, C., 2013. Using agroecosystem modeling to improve the estimates of N_2O emissions in the life-cycle assessment of biofuels. Waste Biomass Valor. 4, 593–606.

DüV, Verordnung über die Anwendung von Düngemitteln, Bodenhilfsstoffen, Kultursubstraten und Pflanzenhilfsmitteln nach den Grundsätzen der guten fachlichen Praxis beim Düngen (Düngeverordnung – DüV, German legislation on fertilization). Bundesgesetzblatt Jahrgang 2006 Teil I Nr. 2, 2006.

EU, 2015. Directive (EU) 2015/1513 of the European Parliament and of the Council of 9 September 2015 amending Directive 98/70/EC relating to the quality of petrol and diesel fuels and amending Directive 2009/28/EC on the promotion of the use of energy from renewable sources. Off. J. Eur. Union L 239, 1.

Edwards, R., Mulligan, D., Giuntoli, J., Agostini, A., Boulamanti, A., Koeble, R., Marelli, L., et al., 2013. Assessing GHG Default Emissions from Biofuels in EU Legislation. Review of Input Database to Calculate Default GHG Emissions, Following Expert Consultation 22–23 November 2011, Ispra (Italy). JRC Scientific and Policy Reports. EUR 25595 EN. European Commission Joint Research Centre Institute for Energy and Transporthttp://dx.doi.org/10.2788/66442.

Edwards, R., O'Connell, A., Padella, M., Mulligan, D., Giuntoli, J., Agostini, A., Koeble, R., Moro, A., Marelli, L., 2016. Definition of Input Data to Assess GHG Default Emissions from Biofuels in EU Legislation, JRC Science for Policy Report EUR 26853 EN.

Escobar, L.F., Amado, T.J.C., Bayer, C., Chavez, L.F., Zanatta, J.A., Fiorin, J.E., 2010. Postharvest nitrous oxide emissions from a subtropical oxisol as influenced by summer crop residues and their management. Rev. Bras. Cienc. Solo 34, 435–442.

FAO, 2016. http://faostat3. fao.org/download/Q/QC/E. (Accessed 29.09.2016).

Flessa, H., Dörsch, P., Beese, F., 1995. Seasonal variation of N_2O and CH_4 fluxes in differently managed arable soils in southern Germany. J. Geophys. Res. 100, 23115–23124.

Flessa, H., Potthoff, M., Loftfield, N., 2002. Greenhouse estimates of CO_2 and N_2O emissions following surface application of grass mulch: importance of indigenous microflora of mulch. Soil Biol. Biochem. 34, 875–879.

German Federal Statistical Office, 2017, DESTATIS database, www.destatis.de (Accessed 16.02.2017).

Granli, T., Bøckman, O.C., 1994. Nitrous oxide from agriculture. Nor. J. Agric. Sci. (Suppl. 12).

Hamelinck, C., De Loveinfosse, I., Koper, M., et al., 2013. Renewable Energy Progress and Biofuels Sustainability. Ecofys, London.

Hegewald, H., Koblenz, B., Wensch-Dorendorf, M., Christen, O., 2016. Impacts of high intensity crop rotation and N management on oilseed rape productivity in Germany. Crop Pasture Sci. 67, 439–449.

Henke, J., Breustedt, G., Sieling, K., Kage, H., 2007. Impact of uncertainty on the optimum nitrogen fertilization rate and agronomic, ecological and economic factors in an oilseed rape based crop rotation. J. Agric. Sci. 145, 455–468.

Hoben, J.P., Gehl, R.J., Millar, N., Grace, P.R., Robertson, G.P., 2011. Nonlinear nitrous oxide (N_2O) response to nitrogen fertilizer in on-farm corn crops of the US Midwest. Gobal Change Biol. 17, 1140–1152.

Honaker, J., King, G., Blackwell, M., 2011. Amelia II: a program for missing data. J. Stat. Softw. 45, 1–47.

Hong, J., 2012. Uncertainty propangation in life cycle assesment of biodiesel versus diesel: global warming and non-renewable energy. Bioresour. Technol. 113, 3–7.

Huber, P.J., 1981. Robust Statistics. Wiley.

Hutchinson, G.L., Livingston, G.P., 2001. Vents and seals in non-steady-state chambers used for measuring gas exchange between soil and the atmosphere. Eur. J. Soil Sci. 52, 675–682.

Hutchinson, G.L., Mosier, A.R., 1981. Improved soil cover method for field measurement of nitrous oxide fluxes. Soil Sci. Soc. Am. J. 45, 311–316.

IPCC, et al., 2006. IPCC. In: Egglestone (Ed.), Guidelines for National Greenhouse Gas Inventories. Prepared by the National Greenhouse Gas Inventories Programme. IGES, Japan.

IPCC, 2013. Summary for policymakers. In: Stocker, T.F., Qin, D., Plattner, G.-K., Tignor, M., Allen, S.K., Boschung, J., Nauels, A., Xia, Y., Bex, V., Midgley, P.M. (Eds.), Climate Change 2013: The Physical Science Basis. Contribution of Working Group I to the Fifth Assessment Report of the Intergovernmental Panel on Climate Change. Cambridge University Press, Cambridge, United Kingdom and New York, NY USA, pp. 1–27.

IPCC,, 2001. Climate change 2001: the scientific basis. In: Houghton, J.T., Ding, Y., Griggs, D.J., Noguer, M., van der Linden, P.J., Dai, X., Maskell, K., Johnson, C.A. (Eds.), Contribution of Working Group I to the Third Assessment Report of the Intergovernmental Panel on Climate Change. Cambridge University Press Cambridge, United Kingdom and New York, NY USA.

IUSS Working Group, 2015. World Reference Base for Soil Resources 2014, Update 2015. International Soil Classification System for Naming Soils and Creating Legends for Soil Maps. World Soil Resources Reports No. 106. FAO, Rome.

Jamali, H., Quale, W., Scheer, C., Rowlings, D., Baldock, J., 2016. Effect of soil texture and wheat plants on N_2O fluxes: a lysimeter study. Agric. For. Meteorol. 223, 17–29.

Jones, S.K., Rees, R.M., Skiba, U.M., Ball, B.C., 2007. Influence of organic and mineral N fertiliser on N_2O fluxes from a temperate grassland. Agric. Ecosyst. Environ. 121, 74–83.

Jungkunst, H.F., Freibauer, A., Neufeldt, H., Bareth, G., 2006. Nitrous oxide emissions from agricultural land use in Germany— a synthesis of available annual field data. J. Plant Nutr. Soil Sci. 169, 341–351.

Kaiser, E.A., Ruser, R., 2000. Nitrous oxide emissions from arable soils in Germany – an evaluation of six long-term field experiments. J. Plant Nutr. Soil Sci. 163, 249–260.

Kammann, C., Grünhage, L., Müller, C., Jacobi, S., Jäger, H.J., 1998. Seasonal variability and mitigation options for N_2O emissions from differently managed grasslands. Environ. Pollut. 102, 179–186.

Kim, D.-G., Hernandez-Ramirez, G., Giltrap, D., 2013. Linear and nonlinear dependency of direct nitrous oxide emissions on fertilizer nitrogen input: a meta-analysis. Agric. Ecosyst. Environ. 168, 53–65.

Kreyling, J., Henry, H.A.L., 2011. Vanishing winters in Germany: soil frost dynamics and snow cover trends: and ecological implications. Clim. Res. 46, 269–276.

Kuznetsova, A., Bruun Brockhoff, P., Bojesen Christensen, R.H., 2016. LmerTest: Tests in Linear Mixed Effects Models. R Package Version 2. pp. 0–32. https://CRAN.R-project.org/package=lmerTest.

Laville, P., Lehuger, S., Loubet, B., Chaumartin, F., Cellier, P., 2011. Effect of management, climate and soil conditions on N_2O and NO emissions from an arable crop rotation using high temporal resolution measurments. Agric. For. Meteorol. 151, 228–240.

Le Gall, C., Jeuffroy, M.H., Hénault, C., Phyton, Y., Cohan, J.P., Parnaudeau, V., Mary, B., Compere, P., Tristant, D., Duval, R., Cellier, P., 2014. Analyser et estimer les émissions de N_2O dans les systèmes de grande cultures francais. Innov. Agronomiques 34, 97–112.

Müller, T., Magid, J., Jensen, L.S., Nielsen, N.E., 2003. Decomposition of plant residues of

different quality in soil—DAISY model calibration and simulation based on experimental data. Ecol. Model. 166, 3–18.
MacKenzie, A.F., Fan, M.X., Cadrin, F., 1997. Nitrous oxide emission as affected by tillage, corn-soybean-alfalfa and nitrogen fertilization. Can. J. Soil Sci. 77, 145–152.
Maidl, F.-X., Limbrunner, B., 2008. So optimieren Sie Ihre N-Düngung in Raps (Publication in german). Top Agrar 2 (2008), 64–66.
Malagoli, P., Laine, P., Rossato, L., Ourry, A., 2005. Dynamics of nitrogen uptake and mobilization in field grown winter oilseed rape (Brassica napus) from stem extension to harvest. 1. Global N flows between vegetative and reproductive tissues I relation to leaf fall and their residueal. N. Ann. Bot. 95, 853–861.
McSwiney, C.P., Robertson, G.P., 2005. Nonlinear response of N_2O flux to incremental fertilizer addition in a continous maize (Zea mays L.) cropping system. Gobal Change Biol. 11, 1712–1719.
Meier, U., 2001. Growth Stages of Mono- and Dicotyledonous Plants. BBCH Monograph, 2nd ed. Federal Biological Research Centre for Agriculture and Forestry, Braunschweig.
Mosier, A.R., Parton, W.J., Hutchinson, G.L., 1983. Modelling nitrous oxide evolution from cropped and native soils. In: Hallberg, R. (Ed.), Environmental Biogeochemistry. Ecological Bulletin, Stockholm, pp. 229–241.
Nett, L., Fuß, R., Flessa, H., Fink, M., 2015. Emissions of nitrous oxide and ammonia from a sandy soil following surface application and incorporation of cauliflower leaf residues. J. Agric. Sci. 153, 1341–1352.
Pedersen, A.R., Petersen, S.O., Schelde, K., 2010. A comprehensive approach to soil-atmosphere trace-gas flux estimation with static chambers. Eur. J. Soil Sci. 61, 888–902.
Pelster, D.E., Chatigny, M.H., Rochette, P., Angers, D.A., Rieux, C., Vanasse, A., 2012. Nitrous oxide emissions respond differently to mineral and organic nitrogen sources in contrasting soil types. J. Environ. Qual. 41, 427–435.
Pfab, H., Palmer, I., Buegger, F., Fiedler, S., Müller, T., Ruser, R., 2011. N_2O fluxes from a Haplic Luvisol under intensive production of lettuce and cauliflower as affected by different N fertilization strategies. J. Plant Nutr. Soil Sci. 174, 545–553.
R Core Team, 2016. R: A language and environment for statistical computing. R Foundation for Statistical Computing, Vienna, Austria.
Röver, M., Heinemeyer, O., Kaiser, E.A., 1998. Microbial induced nitrous oxide emissions from an arable soil during winter. Soil Biol. Biochem. 14, 1859–1865.
RED, 2009. 28/EC of the European Parliament and of the Council of 23 April 2009 on the promotion of the use of energy from renewable sources and amending and subsequently repealing Directives 2001/77/EC and 2003/30/EC. Off. J. Eur. Union 140, 16–45.
Rathke, G.-W., Behrens, T., Diepenbrock, W., 2006. Integrated nitrogen management strategies to improve seed yield, oil content and nitrogen efficiency of winter oilseed rape (Brassica napus L.): a review. Agric. Ecosyst. Environ. 117, 80–108.
Ravishankara, A.R., Daniel, J.S., Portman, R.W., 2009. Nitrous oxide (N_2O): The dominant ozone-depleting substance emitted in the 21st century. Science 326, 123–125.
Reeves, S., Wang, W., 2015. Optimum sampling time and frequency for measuring N_2O emissions from a rain-fed cereal cropping system. Sci. Total Environ. 530–531, 219–226.
Risk, N., Snider, D., Wagner-Riddle, C., 2013. Mechanisms leading to enhanced soil nitrous oxide fluxes induced by freeze-thaw cycles. Can. J. Soil Sci. 93, 401–414.
Ruser, R., Flessa, H., Schilling, R., Steindl, H., Beese, F., 1998. Soil compaction and fertilization effects on nitrous oxide and methane fluxes in potato fields. Soil Sci. Soc. Am. J. 62, 1587–1595.
Ruser, R., Flessa, H., Schilling, R., Beese, F., Munch, J.C., 2001. Effect of crop-specific field management and N fertilization on N_2O emissions from a fine-loamy soil. Nutr Cycl. Agroecosyst. 59, 177–191.
Satterthwaite, F.E., 1946. An approximate distribution of estimates of variance components. Biomet. Bull. 2, 110–114.
Sehy, U., Ruser, R., Munch, J.C., 2003. Nitrous oxide fluxes from maize fields: relationship to yield, site-specific fertilization, and soil conditions. Agric. Ecosyst. Environ. 99, 97–111.
Shaw, L.J., Nicol, G.W., Smith, Z., Fear, J., Prosser, J.I., Baggs, E.M., 2006. Nitrosospira spp. can produce nitrous oxide via a nitrifier denitrification pathway. Environ. Microbiol. 8, 214–222.
Shcherbak, I., Millar, N., Robertson, G.P., 2014. Global metaanalysis of the nonlinear response of soil nitrous oxide (N_2O) emissions to fertilizer nitrogen. PNAS 111, 9199–9204.
Sieling, K., Kage, H., 2010. Efficient N management using winter oilseed rape. A review. Agron. Sustain. Dev. 30, 271–279.
Smith, K.A., Searchinger, T.D., 2012. Crop-based biofuels and associated environmental concerns. Glob. Change Biol. Bioenergy 4, 479–484.
Smith, K.A., McTaggart, I.P., Dobbie, K.E., Conen, F., 1998. Emissions of N_2O from Scottish agricultural soils, as a function of fertilizer N. Nutr. Cycl. Agroecosyst. 52, 123–130.
Stehfest, E., Bouwman, A.L., 2006. N_2O and NO emission from agricultural fields and soils under natural vegetation: summarizing available measurement data and modeling of global annual emissions. Nutr. Cycl. Agroecosyst. 74, 207–228.
Sylvester-Bradley, R., Thorman, R.E., Kindred, D.R., Wynn, S.C., Smith, K.E., Rees, R.M., Topp, C.F.E., Pappa, V.A., Mortimer, N.D., Misselbrook, T.H., Gilhespy, S., Cardenas, L.M., Chauhan, M., Bennett, G., Malkin, S., Munro, D.G., 2015. Minimising Nitrous Oxide Intensities of Arable Crop Products. AHDB Cereals & Oils Project Report No. 548.
Syp, A., Faber, A., Kozak, M., 2016. Assessment of N_2O emissions from rapeseed cutlivation in Poland by various approaches. Int. Agrophys. 30, 501–507.
Teepe, R., Vor, A., Beese, F., Ludwig, A., 2004. Emissions of N_2O from soils during cycles of freezing and thawing and the effects of soil water texture, and duration of freezing. Eur. J. Soil Sci. 55, 357–365.
Van Groenigen, J.W., Kasper, G.J., Velthof, G.L., van den Pol-van Dasselaar, A., Kuikman, P.J., 2004. Nitrous oxide emissions from silage maize fields under different mineral nitrogen fertilizer and slurry applications. Plant Soil 263, 101–111.
Van Groenigen, J.W., Velthof, G.L., Oenema, O., van Groenigen, K.J., van Kessel, C., 2010. Towards an agronomic assessment of N_2O emissions. A case study for arable crops. Eur. J. Soil Sci. 61, 903–913.
WMO, 2016. The state of greenhouse gases in the atmosphere based on global observations through 2015. Greenh. Gas Bull. 12, 1–8.
Wagner-Riddle, C., Furon, A., McLaughlin, N.L., Lee, I., Barbeau, J., Jayasundara, S., Parkin, G., von Bertoldi, P., Warland, J., 2007. Intensive measurement of nitrous oxide emissions from a corn-soybean-wheat rotation under two contrasting management systems over 5 years. Global Chance Biol. 13, 1722–1736.
Walter, K., Don, A., Fuß, R., Kern, J., Drewer, J., Flessa, H., 2015. Direct nitrous oxide emissions from oilseed rape cropping – a meta-analysis. Glob. Change Biol. Bioenergy 7, 1260–1271.
Wood, S.N., 2011. Fast stable restricted maximum likelihood and marginal likelihood estimation of semiparametric generalized linear models. J. R. Stat. Soc. B 73, 3–36.
Wrage, N., Velthof, G.L., van Beusichem, M.L., Oenema, O., 2001. Role of nitrifier denitrification in the production of nitrous oxide. Soil Biol. Biochem. 33, 1723–1732.
Xu, X.K., Duan, C.T., Wu, H.H., Li, T.S., Cheng, W.G., 2016. Effect of intensity and duration of freezing on soil microbial biomass extractable C and N pools, and N_2O and CO_2 emissions from a forest soil in cold temperate region. Sci. China Earth Sci. 59, 156–169.
Zebarth, B.J., Rochette, P., Burton, D.L., 2008. N_2O emissions from spring barley production as influenced by fertilizer nitrogen rate. Can. J. Soil Sci. 88, 197–205.